

Predicting Drug–Drug Interactions Between Rifampicin and Long-Acting Cabotegravir and Rilpivirine Using Physiologically Based Pharmacokinetic Modeling

Rajith K. R. Rajoli,¹ Paul Curley,¹ Justin Chiong,¹ David Back,¹ Charles Flexner,² Andrew Owen,¹ and Marco Siccardi¹

¹ Department of Molecular and Clinical Pharmacology, University of Liverpool, United Kingdom; and ² Johns Hopkins University School of Medicine and Bloomberg School of Public Health, Baltimore, Maryland

Background. Cabotegravir and rilpivirine are 2 long-acting (LA) antiretrovirals that can be administered intramuscularly; their interaction with rifampicin, a first-line antituberculosis agent, has not been investigated. The aim of this study was to simulate and predict drug–drug interactions (DDIs) between these LA antiretroviral agents and rifampicin using physiologically based pharmacokinetic (PBPK) modeling.

Methods. The designed PBPK models were qualified (according to European Medicines Agency guidelines) against observed data for oral formulations of cabotegravir, rilpivirine, and rifampicin. Induction potential of rifampicin was also qualified by comparing the DDI between oral cabotegravir and oral rilpivirine with rifampicin. Qualified PBPK models were utilized for pharmacokinetic prediction of DDIs.

Results. PBPK models predicted a reduction in both area under the curve ($AUC_{0-28 \text{ days}}$) and trough concentration ($C_{\text{trough}, 28 \text{th day}}$) of LA cabotegravir of 41%–46% for the first maintenance dose coadministered with 600 mg once-daily oral rifampicin. Rilpivirine concentrations were predicted to decrease by 82% for both $AUC_{0-28 \text{ days}}$ and $C_{\text{trough}, 28 \text{th day}}$ following the first maintenance dose when coadministered with rifampicin.

Conclusions. The developed PBPK models predicted the theoretical effect of rifampicin on cabotegravir and rilpivirine LA intramuscular formulations. According to these simulations, it is likely that coadministration of rifampicin with these LA formulations will result in subtherapeutic concentrations of both drugs.

Keywords. PBPK modeling; cabotegravir; rifampicin; long-acting; drug–drug interaction.

Tuberculosis (TB) and human immunodeficiency virus (HIV) are global epidemics, and individuals who are HIV infected are at high risk of acquiring TB. In 2016, an estimated 1 million individuals infected with TB were coinfecting with HIV, and TB was the leading infectious cause of death in HIV-infected patients [1]. Since the commencement of the global epidemic of HIV, 25% of the 39 million HIV-infected individuals have died due to TB coinfection [2]. HIV accelerates the usual slow progression of TB infection, leading to a significantly higher mortality [3]. Appropriate treatment and care of TB patients with HIV can reduce the risk of mortality and improve survival [4].

Existing antiretrovirals (ARVs) provide successful treatment against HIV. However, in HIV-infected individuals infected

with TB, it is the TB treatment that is often prioritized. Some studies suggest that a longer treatment duration (>8 months) of rifamycins is necessary in HIV-infected individuals compared with the standard regimen in HIV-uninfected individuals (6 months) to lower the risk of TB relapse [5, 6]. Clinical data on drug–drug interactions (DDIs) between ARVs and anti-TB agents often restrict recommended dosing regimens prescribed during coinfection. Even though in vitro data have been used to characterize DDIs in the absence of clinical data, this approach may lead to suboptimal predictions [7].

Nanoformulated cabotegravir and rilpivirine have entered phase 3 combination trials, and a single intramuscular (IM) injection of cabotegravir can result in detectable plasma concentrations for >1 year after a single dose [8]. Studies with cabotegravir and rilpivirine long-acting injectable (LAI) formulations have shown that the combination of these 2 drugs successfully suppresses HIV type 1 virus in humans with monthly or bimonthly IM administration [9]. Cabotegravir is a substrate of uridine glucuronosyl transferase (UGT1A1 and UGT1A9); rilpivirine is a substrate of cytochrome P450 (CYP) 3A4 [8]. Rifampicin is an inducer of both CYP and UGT enzymes [10]. Coadministration of rifampicin with cabotegravir and rilpivirine LAI formulations has not been studied previously. The

Received 4 October 2018; editorial decision 10 December 2018; accepted 17 December 2018; published online December 19, 2018.

Presented in part: Conference on Retroviruses and Opportunistic Infections, Boston, Massachusetts, 4–7 March 2018. Poster 497.

Correspondence: M. Siccardi, PhD, Department of Molecular and Clinical Pharmacology, University of Liverpool, 70 Pembroke Place, Liverpool L69 3GF, UK (siccardi@liverpool.ac.uk).

The Journal of Infectious Diseases® 2019;219:1735–42

© The Author(s) 2018. Published by Oxford University Press for the Infectious Diseases Society of America. All rights reserved. For permissions, e-mail: journals.permissions@oup.com. DOI: 10.1093/infdis/jiy726

clinical investigation of DDIs for LAI therapy is complicated by challenges in discontinuing the drug administration, hindering the feasibility of future studies.

Physiologically based pharmacokinetic (PBPK) modeling is a bottom-up approach in which drug physicochemical data (eg, log P, pKa, polar surface area, and hydrogen bond donors), in vitro data (eg, intrinsic clearance, blood-to-plasma ratio, protein binding), and systemic data (anatomical, physiological, and demographic) are converted to mathematical equations to describe key pharmacokinetic processes—absorption, distribution, metabolism, and excretion—in humans [11]. This type of modeling can predict DDIs in the absence of clinical study data, and is currently used in drug development and optimization of clinical dosing scenarios. PBPK modeling is also being considered as an alternative to human trials to explore DDIs that are complex and difficult to study in patient populations [12].

The aim of this study was to develop a PBPK model to simulate the DDIs between the LAI cabotegravir and rilpivirine and rifampicin in virtual healthy individuals. The designed PBPK models were qualified against observed data for the induction potential of rifampicin on hepatic metabolism. The qualified models were used to predict the DDI potential between oral rifampicin and existing LAI cabotegravir and rilpivirine formulations.

METHODS

A cohort of 100 healthy virtual individuals (50% female) were generated with a whole-body PBPK model, designed using Simbiology version 4.3.1., a product of MATLAB version 8.2 (MathWorks, Natick, Massachusetts) [13]. The following assumptions have been made during simulations: (1) Drug distribution was described using blood flow-limited first-order kinetics [14]; (2) instant and uniform drug distribution

(well-stirred model) occurred across each tissue and organ; and (3) there was no drug reabsorption from the colon. Ethical approval was not necessary for this study as the data were computer generated.

Anatomy and Physiology

Virtual adults aged 18–60 years, weighing between 40 and 100 kg (77 ± 15 kg) and having a height between 1.5 and 2.0 m ($1.75 \pm .17$ m), were considered for this study. Organ, tissue weights, and blood flow rates were computed using various anthropometric equations from previous publication [15]. The model has an in-built function that generates random values based on described mean and standard deviation, such that no 2 simulated individuals have the same characteristics, thus generating a virtual population of individuals.

Oral absorption was based on a 7-compartment absorption and transit model [16]. Drug absorption rate through the small intestine was computed using either apparent permeability in Caco-2 cells or molecular properties: polar surface area (expressed as Å) and number of hydrogen bond donors [17]. Drug physicochemical parameters are presented in Table 1. The absorption model assumes that drug is in solution, readily available for absorption, and does not account for solubility.

Drug intrinsic clearance values obtained from in vitro experiments conducted in human liver microsomes and recombinant enzymes, along with total enzyme abundance in the liver, were used to compute intestinal metabolism, first-pass metabolism, and systemic clearance [17].

CYP3A4 induction by rifampicin was introduced in the gut during intestinal metabolism and in the liver for hepatic metabolism whereas UGT induction was considered only in the liver. The rifampicin CYP induction model was obtained from a previous publication [29] as indicated:

Table 1. Physicochemical Properties and In Vitro and Population Pharmacokinetic Data of Cabotegravir, Rilpivirine, and Rifampicin

Property	Cabotegravir	Rilpivirine	Rifampicin
Molecular weight	427	366	823
Log P _{ow}	1.04 [18]	4.32 [19]	2.7 [20]
Protein binding	99.3% [21]	99.7% [19]	80.0% [22]
pK _a	10.04 [18]	3.26 [19]	1.7 [20]
R	.441 [23]	.67 [19]	.9 [24]
Polar surface area	99.2	97.42	220.15
Hydrogen bond donors	2	2	6
Caco-2 permeability, cm/sec	Not available	12×10^{-6} [19]	5.79×10^{-6} [25]
Apparent clearance, L/h	NA	NA	10.3 (7.49–12.0) [26]
CYP3A4, CL _{int}	NA	2.04 [19]	NA
UGT1A1, CL _{int}	4.5 [27]	NA	NA
UGT1A9, CL _{int}	2.2 [27]	NA	NA
Release rate, h ⁻¹	4.5×10^{-4} [28]	9×10^{-4} [8]	NA
Ind _{max} /Ind ₅₀ CYP3A4	NA	NA	15/.715 [29]
UGT clearance	NA	NA	↑2.4 fold [10]

Abbreviations: CL_{int}, intrinsic clearance; CYP, cytochrome P450 (μL/minute/pmol); Ind₅₀, 50% maximal induction; Ind_{max}, maximum induction potential; log P_{ow}, partition coefficient between octanol and water; NA, not applicable; pKa, logarithmic value of the dissociation constant; R, blood-to-plasma drug ratio; UGT, uridine diphosphate glucuronosyltransferase (μL/minute/mg).

$$CYP = CYP_0 \left(1 + \frac{Ind_{max} \times RIF}{IC_{50} + RIF} \right),$$

where CYP is the enzyme level at time t ; CYP_0 is the enzyme level at time $t = 0$, subsequent to rifampicin administration; Ind_{max} is the maximum induction potential; IC_{50} is the induction potential at 50% maximum; and RIF is the concentration of rifampicin at time t .

Drug disposition through organs and tissues was described using first-order differential equations [30], and the volume of distribution was computed using drug physicochemical parameters and tissue-to-plasma ratio [31]. An additional compartment was appended to describe the IM depot and drug disposition from muscle to the surrounding blood capillaries. Concentration dependent first-order passive diffusion was assumed, and no transporters were considered in the model [32].

Model Qualification

Model qualification was performed according to the European Medicines Agency (EMA) guidelines [33]. The models were assumed to be qualified if the difference between mean simulated pharmacokinetic parameters (maximum concentration [C_{max}], area under the curve [AUC], and trough concentration [C_{trough}]) was <2-fold from the observed mean. The pharmacokinetic data comparing observed and simulated data and also the pharmacokinetic curves are recorded in [Supplementary Tables 1 and 2](#) and [Supplementary Figures 1–3](#).

Oral Administration of Rilpivirine, Cabotegravir, and Rifampicin

The PBPK model was initially qualified against available oral data. A single oral dose of cabotegravir 30 mg [10] and oral doses of 25 mg and 150 mg once-daily (OD) rilpivirine at steady-state were qualified against observed data [34]. The rilpivirine oral 150 mg model was also qualified since this dose was used in the drug interaction study with 600 mg OD rifampicin. The rifampicin 600 mg OD oral dose was qualified against observed data at day 6 and day 14 to capture the induction potential [29].

Drug–Drug Interaction

The drug interaction between 30 mg oral cabotegravir and 600 mg OD oral rifampicin was compared against observed data. The simulations were conducted according to the reported study design with the administration of OD rifampicin for 21 days and simultaneous administration of a single dose of oral cabotegravir on day 14. The effect was compared against oral cabotegravir when administered alone (30 mg) [10].

Simultaneous administration of oral rifampicin 600 mg OD and oral rilpivirine 150 mg OD for 7 days was simulated, analogous to the reported study, and the data were compared against observed data [34]. The effect of rifampicin on oral rilpivirine was compared with drug administered alone.

Intramuscular Administration of Cabotegravir and Rilpivirine

Pharmacokinetic curves of both IM loading doses (LDs) and IM maintenance doses (MDs) of cabotegravir and rilpivirine were validated against data from the long-acting antiretroviral treatment enabling (LATTE-2) studies [9]. The IM LDs of 800 mg and 900 mg were preceded by oral doses of 30 mg and 25 mg for cabotegravir and rilpivirine, respectively, ([Figure 1](#)). Monthly/bimonthly doses of 400/600 mg for cabotegravir and 600/900 mg for rilpivirine were simulated. Plasma concentration vs time plots were compared against observed data from literature [9] and presented in [Supplementary Figures 1–3](#).

Model Prediction

Drug–drug interactions between oral rifampicin and IM LAIs of cabotegravir and rilpivirine were simulated. Oral dosing of 30 mg cabotegravir/25 mg rilpivirine was followed by IM LD of 800 mg cabotegravir/900 mg rilpivirine and IM MDs ([Figure 1](#)). Throughout this dosing regimen, oral 600 mg OD rifampicin was administered. Simulations of monthly IM LA cabotegravir were also conducted up to week 86. Rifampicin was coadministered from weeks 56 to week 80 and the pharmacokinetics were compared with cabotegravir alone.

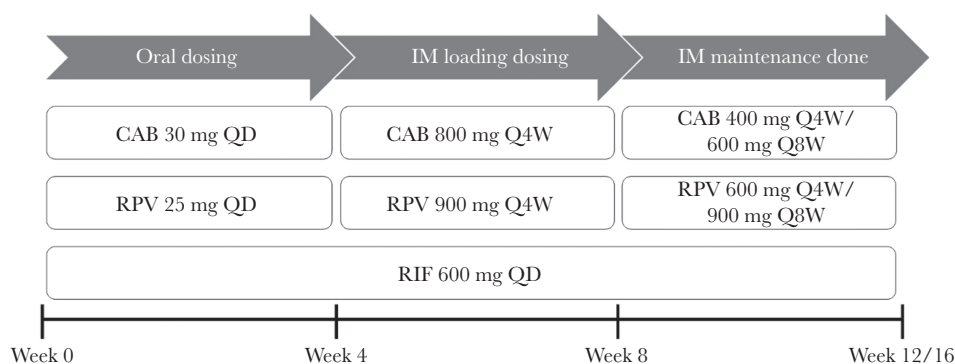


Figure 1. Dosing regimen followed to simulate the effect of rifampicin on intramuscular cabotegravir and rilpivirine. Abbreviations: CAB, cabotegravir; IM, intramuscular; Q4W, once every 4 weeks; Q8W, once every 8 weeks; QD, once daily; RIF, rifampicin; RPV, rilpivirine.

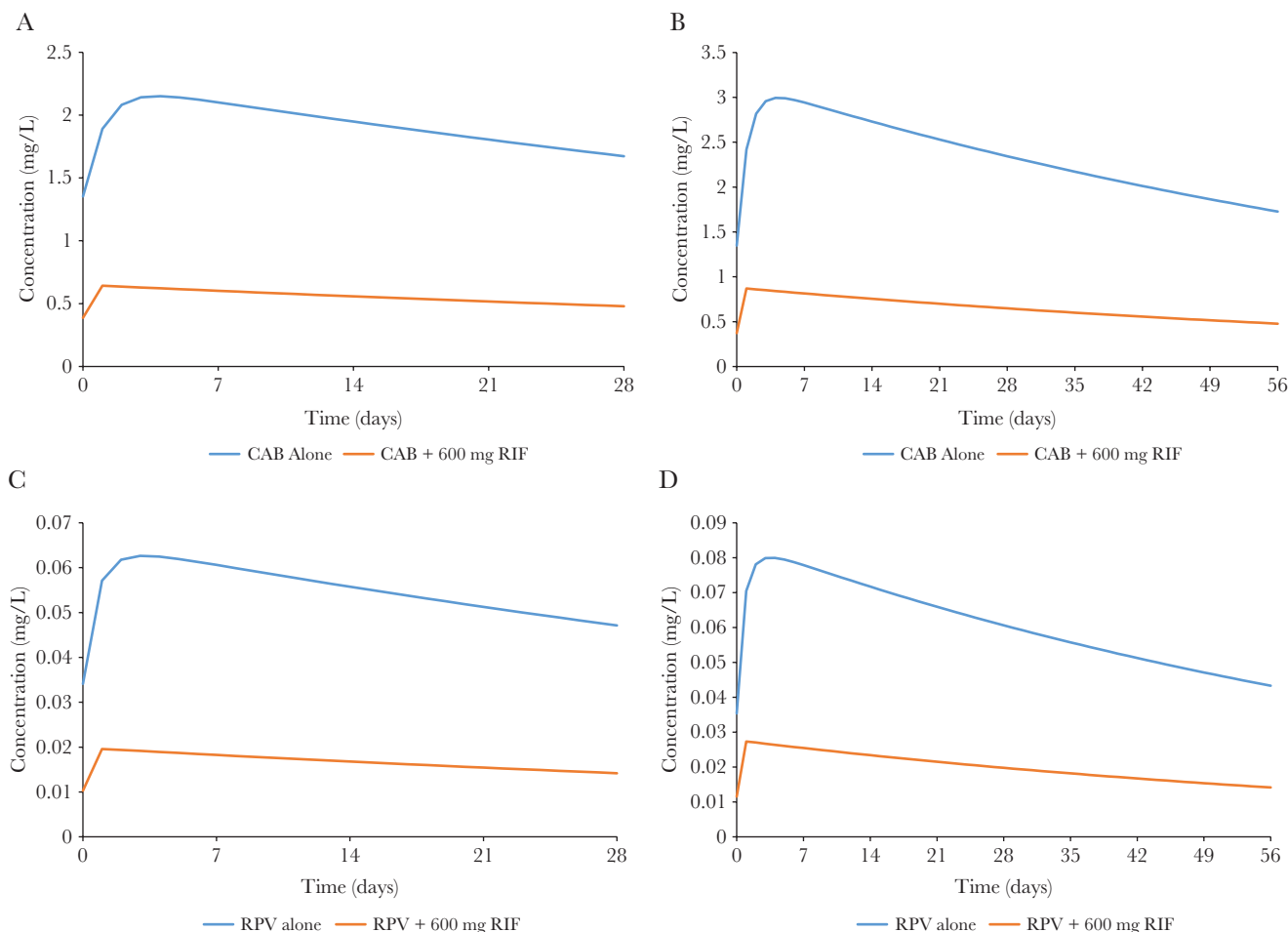


Figure 2. Pharmacokinetic decay of long-acting intramuscular maintenance doses of cabotegravir and rilpivirine with and without 600 mg once-daily rifampicin. *A*, 400 mg cabotegravir every 4 weeks. *B*, 600 mg cabotegravir every 8 weeks. *C*, 600 mg rilpivirine every 4 weeks. *D*, 900 mg rilpivirine every 8 weeks. Abbreviations: CAB, cabotegravir; RIF, rifampicin; RPV, rilpivirine.

RESULTS

Model Qualification

The comparison of the simulated pharmacokinetic parameters and observed data of oral cabotegravir, rilpivirine, and rifampicin are shown in [Supplementary Table 1](#). The differences between the mean simulated C_{max} , AUC, and C_{trough} values was <2-fold and were comparable to the observed data; therefore, the designed PBPK models were assumed to be qualified. The simulated AUC_{0-24h} of rifampicin on day 6 and day 14 was $66.2 \text{ mg} \times \text{hour/L}$ and $63.3 \text{ mg} \times \text{hour/L}$, respectively, and was comparable to the observed values of $99.8 \text{ mg} \times \text{hour/L}$ and $70.3 \text{ mg} \times \text{hour/L}$, respectively [29]. Pharmacokinetic plasma concentration vs time plots of the qualification are presented in [Supplementary Figures 1–3](#).

Simulated DDIs between 30 mg oral OD cabotegravir and 600 mg oral OD rifampicin resulted in a decrease in C_{max} , AUC_{0-24h} , and $C_{trough, 24h}$ of 10.2%, 59.9%, and 49.7%, respectively, and were comparable to the observed values of 6.1%, 59.1%, and 50.6%, respectively [10] ([Supplementary Table 2](#)). Similarly, for 150 mg

oral OD rilpivirine with 600 mg oral OD rifampicin, a decrease of 83%, 89.7%, and 93.7% in C_{max} , AUC_{0-24h} , and $C_{trough, 24h}$ was simulated as opposed to the observed values of 69%, 80%, and 89%, respectively [34].

Model Prediction

Model predictions of DDIs between IM LA ARVs and rifampicin are presented in [Table 2](#) and [Figure 2](#). The simulated DDI between 400 mg IM MD of cabotegravir administered every 4 weeks and 600 mg OD oral rifampicin resulted in a decrease of 41% in both $AUC_{0-28 \text{ days}}$ and $C_{trough, 28th \text{ day}}$ values. For 600 mg MD of cabotegravir administered with rifampicin, a decrease of 46% was observed for both $AUC_{0-56 \text{ days}}$ and $C_{trough, 56th \text{ day}}$ values compared with drug administered alone. Rilpivirine when administered with rifampicin resulted in a simulated decrease of both $AUC_{0-28 \text{ days}}$ and $C_{trough, 28th \text{ day}}$ of 82% for 600 mg IM MD every 4 weeks and 83% for both $AUC_{0-56 \text{ days}}$ and $C_{trough, 56th \text{ day}}$ for a 900 mg IM MD every 8 weeks. For both cabotegravir and rilpivirine DDIs with rifampicin, there was an 8% decrease in apparent plasma half-lives ([Table 1](#)).

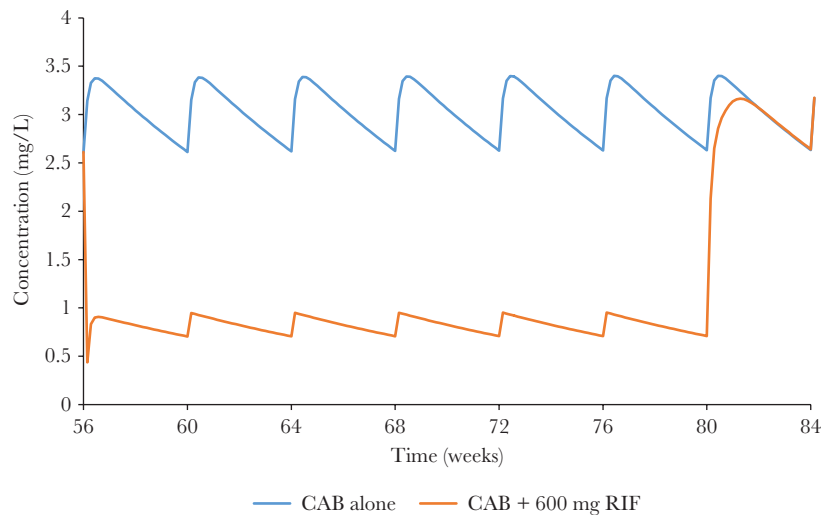


Figure 3. Pharmacokinetics of 400 mg long-acting intramuscular maintenance dose of cabotegravir at steady-state with and without 600 mg once-daily rifampicin. Rifampicin was coadministered from week 56 to week 80. Abbreviations: CAB, cabotegravir; RIF, rifampicin.

Steady-state IM LA cabotegravir when administered with rifampicin had plasma concentrations with C_{max} , AUC at steady state $AUC_{ss,56-80th\ week}$ and $C_{trough, 56-80th\ week}$ of .95 mg/L, 1717 mg \times hour/L, and .44 mg/L respectively, compared with 3.40 mg/L, 12 228 mg \times hour/L, and 2.61 mg/L when administered alone between the weeks of 56 and 80, with a simulated decrease in C_{max} , $AUC_{ss,56-80th\ week}$, and $C_{trough, 56-80th\ week}$ of 72%, 86%, and 83.2%, respectively (Figure 3).

DISCUSSION

The investigation of DDIs between ARVs and anti-TB agents is relevant, as HIV-infected individuals coinfecting with TB have risk of treatment failure and the clinical management of therapies is complex. We were able to optimize PBPK models to identify the impact of the DDIs between rifampicin and the LA IM ARVs cabotegravir and rilpivirine. This

study represents a potentially valuable example of the use of PBPK modeling to investigate difficult clinical scenarios through the understanding of molecular processes underpinning pharmacokinetics—that is, physiochemical and/or metabolic processes including enzyme induction and inhibition. Rifampicin induces both CYP and UGT metabolism, and coadministration of the LA ARVs could result in clinically significant DDIs. The interactions between cabotegravir and rifampicin or rilpivirine and rifampicin have been investigated previously, but only for the oral formulations of all 3 drugs [10, 34]. The IM doses and release rates of existing LA formulations of cabotegravir and rilpivirine used in the LATTE-2 phase 2 studies were used to simulate the pharmacokinetic effects of rifampicin [9].

Our simulated results were in agreement with the values reported for the pharmacokinetics of oral and IM formulations.

Table 2. Pharmacokinetic Summary of Drug Alone and Drug–Drug Interaction Between Cabotegravir and Rilpivirine Long-Acting Intramuscular Formulations Versus 600 mg Oral Rifampicin

Drug	Drug Alone		Drug + 600 mg OD Rifampicin		% Difference (Alone vs DDI)		Half-life, d	
	AUC	C_{trough}	AUC	C_{trough}	AUC	C_{trough}	Alone	Drug + Rifampicin
Cabotegravir 400 mg MD (every 4 weeks)	1340 \pm 295	1.40 \pm .31	794 \pm 186	.8 \pm .2	–40.7%	–40.7%	68	65
Cabotegravir 600 mg MD (every 8 weeks)	2291 \pm 541	1.42 \pm .33	1247 \pm 319	.77 \pm .2	–45.6%	–45.8%	69	64
Rilpivirine 600 mg MD (every 4 weeks)	39 313 \pm 22 724	37.3 \pm 22.3	7128 \pm 3128	6.7 \pm 2.9	–81.9%	–82.1%	62	59
Rilpivirine 900 mg MD (every 8 weeks)	59 219 \pm 28 134	37.4 \pm 17.9	10 175 \pm 4464	6.6 \pm 2.9	–82.8%	–82.4%	62	59

Cabotegravir C_{trough} is expressed as mg/L and AUC in mg \times hour/L, respectively; rilpivirine C_{trough} is expressed as ng/mL and AUC in ng \times hour/mL, respectively. Intramuscular maintenance dose was preceded by 4 weeks of daily oral dose (30 mg cabotegravir, 25 mg rilpivirine) and 4 weeks of intramuscular loading dose (800 mg cabotegravir and 900 mg rilpivirine). AUC and C_{trough} values are represented as mean \pm standard deviation.

Abbreviations: AUC, area under the curve; C_{trough} , trough concentration; DDI, drug–drug interaction; MD, maintenance dose; OD, once daily.

The drug interaction between LA cabotegravir and rifampicin can be classified as weak (20%–50% decrease in AUC) and strong between LA rilpivirine and rifampicin (>80% decrease in AUC) according to the US Food and Drug Administration (FDA) [12]. In both these DDIs, 95% of simulated patients were predicted to have C_{trough} values below the average plasma concentrations achieved without a DDI. Cabotegravir concentrations were maintained above the protein binding–adjusted 90% inhibitory concentration (IC_{90}) value of 166 ng/mL [8], whereas rilpivirine concentrations drop further below the protein binding–adjusted IC_{90} value of 12 ng/mL [35]. Conversely, the interaction between LA cabotegravir at steady-state and oral rifampicin resulted in a >80% reduction in AUC, which can be classified as strong. Overall, these predictions would indicate that the coadministration of rifampicin with both LA rilpivirine and cabotegravir results in subtherapeutic concentrations and would likely lead to a recommendation that this coadministration be avoided.

Although there is a >40% reduction in the AUC for cabotegravir and rilpivirine, respectively, the half-lives remained unchanged (Table 2). This could be explained by the occurrence of so-called flip-flop kinetics—a pharmacokinetic phenomenon observed for LA formulations where the drug absorption rate is slower than the overall elimination rate, during which drug elimination is limited by the rate of absorption [36]. As a result, there is an observed decrease in AUC as the elimination rate increases but half-life remains constant. This is in contrast to oral formulations, where half-life decreases as elimination rate increases. This is also in agreement with the difference observed in simulated AUC and half-lives for drug alone and drug with rifampicin.

These models have been successfully qualified against observed data. However, they are associated with some significant limitations. Concentration-dependent induction of UGT enzymes was not available in the literature for these drugs; hence, a constant increase in oral clearance by a factor of 2.4 for cabotegravir was considered in the model [10]. Active transport was not accounted for all the drugs due to limited availability of data with IM formulations. Evidence of granuloma at the injection site could alter drug pharmacokinetics [37], and this was not factored into these models. Lymphatic circulation is preferred by highly lipophilic drugs such as rilpivirine, and that can delay drug absorption, thus altering plasma C_{trough} [32]. The induction effect may vary in different populations, and these models do not consider physiological changes due to conditions such as aging.

PBPK models have been increasingly used to simulate induction and inhibition effects. Studies include the assessment between efavirenz and CYP3A4/CYP2C8 substrates for both induction and inhibitory effects [7], and the interaction between the ARVs darunavir/ritonavir, efavirenz, and etravirine with the antineoplastic agents gefitinib and erlotinib [38].

In a separate study, the static and dynamic inhibitory effect of an anti-TB drug, clofazimine, on CYPs was assessed using CYP2C8, CYP3A4, and CYP2D6 substrates [39]. An efavirenz induction model was qualified against CYP2B6 and CYP3A4 substrates [40]; DDI and dose escalation studies between efavirenz and an LA contraceptive implant, levonorgestrel [41], were also developed. Recently, the EMA and FDA have provided guidelines on using PBPK models to inform clinical scenarios without the need for clinical studies in humans [33, 42].

The presented data have described the DDI between LA IM cabotegravir and rilpivirine with rifampicin. Results from the PBPK models suggest that the coadministration of rifampicin could have a major effect on the pharmacokinetics of rilpivirine and cabotegravir. The predictive value of these results is bolstered by recently completed healthy volunteer DDI studies of rifampicin with the oral formulations of cabotegravir and rilpivirine. As an alternative to rifampicin, rifabutin may be used in this setting as it is a less potent inducer of CYP and UGT enzymes than rifampicin and is well tolerated in patients; however, further studies would be needed for confirmation [43].

CONCLUSIONS

The developed PBPK models simulated the DDIs between the LA IM ARVs cabotegravir and rilpivirine and the anti-TB agent rifampicin. These PBPK models have been qualified against data from existing oral and IM formulations, and for DDIs resulting from the coadministration of oral ARVs with rifampicin. The predicted data suggest that the coadministration of rifampicin with LA IM rilpivirine and cabotegravir could result in subtherapeutic drug concentrations in HIV-infected individuals coinfecting with TB and that these combinations should be avoided.

Supplementary Data

Supplementary materials are available at *The Journal of Infectious Diseases* online. Consisting of data provided by the authors to benefit the reader, the posted materials are not copyedited and are the sole responsibility of the authors, so questions or comments should be addressed to the corresponding author.

Notes

Author contributions. All authors contributed to the overall concept, design, and choice of the drugs to be tested. R. K. R. R. performed the modeling and analysis. R. K. R. R. and M. S. wrote the manuscript with support from D. B., A. O., and C. F. All authors reviewed and contributed to the final manuscript.

Financial support. This work was supported by the National Institute of Allergy and Infectious Diseases of the National Institutes of Health (grant number R24 AI 118397).

Potential conflicts of interest. D. B. has received grants from ViiV, MSD, Janssen, and Gilead, and personal fees from

ViiV, Gilead, and MSD. C. F. has received grants from Gilead Sciences, and personal fees from ViiV Healthcare, Janssen Pharmaceuticals, Merck Laboratories, Mylan Pharmaceuticals, and Cipla Pharmaceuticals; in addition, C. F. has a patent for semi-solid prodrug solid drug nanoparticles pending. A. O. has received grants from Merck, ViiV Healthcare, Janssen, and AstraZeneca; personal fees from Merck and ViiV Healthcare; and nonfinancial support from Janssen; in addition, A. O. has a patent for drug delivery issued, and a patent for drug delivery pending. M. S. reports grants from ViiV and Janssen. All other authors report no potential conflicts. All authors have submitted the ICMJE Form for Disclosure of Potential Conflicts of Interest. Conflicts that the editors consider relevant to the content of the manuscript have been disclosed.

REFERENCES

- World Health Organization. Global tuberculosis report. http://www.who.int/tb/publications/global_report/en/. Accessed 1 August 2018.
- Joint United Nations Programme on HIV/AIDS. Fact sheet. http://www.unaids.org/sites/default/files/media_asset/UNAIDS_FactSheet_en.pdf. Accessed 1 February 2018.
- Zhou J, Elliott J, Li PC, et al. Risk and prognostic significance of tuberculosis in patients from the TREAT Asia HIV observational database. *BMC Infect Dis* **2009**; 9:46.
- Balcha TT, Skogmar S, Sturegård E, Björkman P, Winqvist N. Outcome of tuberculosis treatment in HIV-positive adults diagnosed through active versus passive case-finding. *Glob Health Action* **2015**; 8:27048.
- Ahmad Khan F, Minion J, Al-Motairi A, Benedetti A, Harries AD, Menzies D. An updated systematic review and meta-analysis on the treatment of active tuberculosis in patients with HIV infection. *Clin Infect Dis* **2012**; 55:1154–63.
- Sterling TR, Alwood K, Gachuhi R, et al. Relapse rates after short-course (6-month) treatment of tuberculosis in HIV-infected and uninfected persons. *AIDS* **1999**; 13:1899–904.
- Marzolini C, Rajoli R, Battagay M, Elzi L, Back D, Sicaardi M. Physiologically based pharmacokinetic modeling to predict drug-drug interactions with efavirenz involving simultaneous inducing and inhibitory effects on cytochromes. *Clin Pharmacokinet* **2017**; 56:409–20.
- Spreen W, Williams P, Margolis D, et al. Pharmacokinetics, safety, and tolerability with repeat doses of GSK1265744 and rilpivirine (TMC278) long-acting nanosuspensions in healthy adults. *J Acquir Immune Defic Syndr* **2014**; 67:487–92.
- Margolis DA, Gonzalez-Garcia J, Stellbrink HJ, et al. Long-acting intramuscular cabotegravir and rilpivirine in adults with HIV-1 infection (LATTE-2): 96-week results of a randomised, open-label, phase 2b, non-inferiority trial. *Lancet* **2017**; 390:1499–510.
- Ford SL, Sutton K, Lou Y, et al. Effect of rifampin on the single-dose pharmacokinetics of oral cabotegravir in healthy subjects. *Antimicrob Agents Chemother* **2017**; 61:e00487–17.
- Rajoli RKR, Back DJ, Rannard S, et al. In silico dose prediction for long-acting rilpivirine and cabotegravir administration to children and adolescents. *Clin Pharmacokinet* **2018**; 57:255–66.
- US Food and Drug Administration. Drug development and drug interactions. <http://www.fda.gov/Drugs/DevelopmentApprovalProcess/DevelopmentResources/DrugInteractionsLabeling/ucm080499.htm>. Accessed 27 March 2018.
- Rajoli RK, Back DJ, Rannard S, et al. Physiologically based pharmacokinetic modelling to inform development of intramuscular long-acting nanoformulations for HIV. *Clin Pharmacokinet* **2015**; 54:639–50.
- Nestorov I. Whole body pharmacokinetic models. *Clin Pharmacokinet* **2003**; 42:883–908.
- Bosgra S, van Eijkeren J, Bos P, Zeilmaker M, Slob W. An improved model to predict physiologically based model parameters and their inter-individual variability from anthropometry. *Crit Rev Toxicol* **2012**; 42:751–67.
- Yu LX, Amidon GL. A compartmental absorption and transit model for estimating oral drug absorption. *Int J Pharm* **1999**; 186:119–25.
- Gertz M, Harrison A, Houston JB, Galetin A. Prediction of human intestinal first-pass metabolism of 25 CYP3A substrates from in vitro clearance and permeability data. *Drug Metab Dispos* **2010**; 38:1147–58.
- Chemaxon. Chemicalize.org: properties viewer. <http://www.chemicalize.org/>. Accessed 18 February 2018.
- US Food and Drug Administration, Center for Drug Evaluation and Research. Clinical pharmacology and biopharmaceutics review(s). Application number: 202022Orig1s000. http://www.accessdata.fda.gov/drug-satfda_docs/nda/2011/202022Orig1s000ClinPharmR.pdf. Accessed 17 July 2018.
- DrugBank. Rifampicin. <https://www.drugbank.ca/drugs/DB01045>. Accessed 22 March 2018.
- Trezza C, Ford SL, Spreen W, Pan R, Piscitelli S. Formulation and pharmacology of long-acting cabotegravir. *Curr Opin HIV AIDS* **2015**; 10:239–45.
- Sousa M, Pozniak A, Boffito M. Pharmacokinetics and pharmacodynamics of drug interactions involving rifampicin, rifabutin and antimalarial drugs. *J Antimicrob Chemother* **2008**; 62:872–8.
- A Culp GB, Gould E, Ford S, et al. Metabolism, excretion, and mass balance of the HIV integrase inhibitor, cabotegravir (GSK1265744) in humans. In: 54th Interscience Conference on Antimicrobial Agents and Chemotherapy, Washington, DC, 2014.

24. Loos U, Musch E, Jensen JC, Mikus G, Schwabe HK, Eichelbaum M. Pharmacokinetics of oral and intravenous rifampicin during chronic administration. *Klin Wochenschr* **1985**; 63:1205–11.
25. Biganzoli E, Cavenaghi LA, Rossi R, Brunati MC, Nolli ML. Use of a Caco-2 cell culture model for the characterization of intestinal absorption of antibiotics. *Farmaco* **1999**; 54:594–9.
26. Seng KY, Hee KH, Soon GH, Chew N, Khoo SH, Lee LS. Population pharmacokinetics of rifampicin and 25-deacetyl-rifampicin in healthy Asian adults. *J Antimicrob Chemother* **2015**; 70:3298–306.
27. Reese M FS, Bowers G, Humphreys J, et al. In vitro drug interaction profile of the HIV integrase inhibitor, GSK1265744, and demonstrated lack of clinical interaction with midazolam. In: 15th International Workshop on Clinical Pharmacology of HIV and Hepatitis Therapy, Washington, DC, 2014.
28. Ford SL, Chen J, Lovern M, Spreen W, Kim J. Population PK approach to predict cabotegravir (CAB, GSK1265744) long-acting injectable doses for phase 2b. In: Interscience Conference on Antimicrobial Agents and Chemotherapy, Washington, DC, 2014.
29. Yamashita F, Sasa Y, Yoshida S, et al. Modeling of rifampicin-induced CYP3A4 activation dynamics for the prediction of clinical drug-drug interactions from in vitro data. *PLoS One* **2013**; 8:e70330.
30. Peters SA. Evaluation of a generic physiologically based pharmacokinetic model for lineshape analysis. *Clin Pharmacokinet* **2008**; 47:261–75.
31. Poulin P, Theil FP. Prediction of pharmacokinetics prior to in vivo studies. 1. Mechanism-based prediction of volume of distribution. *J Pharm Sci* **2002**; 91:129–56.
32. Tegenge MA, Mitkus RJ. A physiologically-based pharmacokinetic (PBPK) model of squalene-containing adjuvant in human vaccines. *J Pharmacokinet Pharmacodyn* **2013**; 40:545–56.
33. European Medicines Agency. Guideline on the qualification and reporting of physiologically based pharmacokinetic (PBPK) modelling and simulation. http://www.ema.europa.eu/docs/en_GB/document_library/Scientific_guideline/2016/07/WC500211315.pdf. Accessed 20 June 2018.
34. Ford N, Lee J, Andrieux-Meyer I, Calmy A. Safety, efficacy, and pharmacokinetics of rilpivirine: systematic review with an emphasis on resource-limited settings. *HIV AIDS* **2011**; 3:35–44.
35. Aouri M, Barcelo C, Guidi M, et al. Population pharmacokinetics and pharmacogenetics analysis of rilpivirine in HIV-1-infected individuals. *Antimicrob Agents Chemother* **2017**; 61:e00899–16.
36. Yáñez JA, Remsberg CM, Sayre CL, Forrest ML, Davies NM. Flip-flop pharmacokinetics—delivering a reversal of disposition: challenges and opportunities during drug development. *Ther Deliv* **2011**; 2:643–72.
37. Darville N, van Heerden M, Vynckier A, et al. Intramuscular administration of paliperidone palmitate extended-release injectable microsuspension induces a subclinical inflammatory reaction modulating the pharmacokinetics in rats. *J Pharm Sci* **2014**; 103:2072–87.
38. Moltó J, Rajoli R, Back D, et al. Use of a physiologically based pharmacokinetic model to simulate drug–drug interactions between antineoplastic and antiretroviral drugs. *J Antimicrob Chemother* **2017**; 72:805–11.
39. Sangana R, Gu H, Chun DY, Einolf HJ. Evaluation of clinical drug interaction potential of clofazimine using static and dynamic modeling approaches. *Drug Metab Dispos* **2018**; 46:26–32.
40. Ke A, Barter Z, Rowland-Yeo K, Almond L. Towards a best practice approach in PBPK modeling: case example of developing a unified efavirenz model accounting for induction of CYPs 3A4 and 2B6. *CPT Pharmacometrics Syst Pharmacol* **2016**; 5:367–76.
41. Roberts O, Rajoli RKR, Back DJ, et al. Physiologically based pharmacokinetic modelling prediction of the effects of dose adjustment in drug-drug interactions between levonorgestrel contraceptive implants and efavirenz-based ART. *J Antimicrob Chemother* **2018**; 73:1004–12.
42. US Food and Drug Administration. Clinical drug interaction studies—study design, data analysis, and clinical implications. <https://www.fda.gov/downloads/Drugs/Guidance/ComplianceRegulatoryInformation/Guidances/ucm292362.pdf>. Accessed 1 February 2018.
43. Horne DJ, Spitters C, Narita M. Experience with rifabutin replacing rifampin in the treatment of tuberculosis. *Int J Tuberc Lung Dis* **2011**; 15:1485–9, i.